Distribution of ions near a charged selective surface in critical binary solvents

Alina Ciach[1] and Anna Maciołek[1,2,3]
[1]*Institute of Physical Chemistry, Polish Academy of Sciences, Kasprzaka 44/52, PL-01-224 Warsaw, Poland*
[2]*Max-Planck-Institut für Metallforschung, Heisenbergstr. 3, D-70569 Stuttgart, Germany*
[3]*Institut für Theoretische und Angewandte Physik, Universität Stuttgart, Pfaffenwaldring 57, D-70569 Stuttgart, Germany*
(Received 11 January 2010; published 22 April 2010)

Near-critical binary mixtures containing ionic solutes near a charged wall preferentially adsorbing one component of the solvent are studied. Within the Landau-Ginzburg approach extended to include electrostatic interactions and the chemical preference of ions for one component of the solvent, we obtain a simple form for the leading-order correction to the Debye-Hückel theory result for the charge density profile. Our result shows that critical adsorption influences significantly distribution of ions near the wall. This effect may have important implications for the screening of electrostatic interactions between charged surfaces immersed in binary near-critical solvents.

DOI: 10.1103/PhysRevE.81.041127 PACS number(s): 05.70.Jk, 05.70.Np, 61.20.Qg, 68.35.Rh

I. INTRODUCTION

A phenomenon of critical adsorption occurs when a fluid is brought to its bulk critical point in the presence of an attractive substrate or wall, for example, along the critical isochore. The wall causes a perturbation of the relevant order parameter profile to extend over a distance $\sim\xi_b$, the bulk correlation length, from the surface [1,2]. Close to criticality, where $\xi_b \sim |(T-T_c)/T_c|^{-\nu}$ (ν is the critical exponent), the influence of the wall extends to macroscopic distances. As a result the amount adsorbed (adsorption Γ) diverges as $\tau = (T-T_c)/T_c \to 0$. Here we focus on the equivalent phenomenon that occurs for binary liquid mixtures near their consolute points. In these systems, generically there is a preferential adsorption of one component of the mixture on the wall surfaces, resulting in the divergence of the relative adsorption near the critical point.

Critical adsorption was much studied both theoretically and experimentally. Of interest has been the scaling prediction by Fisher and de Gennes [3] that Γ should have a power law dependence on τ, with a universal exponent which does not depend on the details of the specific system. Also, this phenomenon is of significant practical importance, e.g., for the use of supercritical fluids in micro- and nanofluidics [4] and as solvents in colloidal suspensions [5].

In colloidal suspensions one usually encounters the presence of ions. This may be due to the dissociation of a salt-free solvent, e.g., in binary solvents containing water, or due to dissolved salt. Ions influence the electrostatic interactions between the charged colloids leading to screening effects [6]. If there is a chemical preference of ions for one component of the solvent, then larger amount of ions may be dissolved in regions where the concentration of the preferred component of the solvent is larger. For this reason critical adsorption in binary solvents may affect the distribution of ions near charged surfaces. This effect in turn may influence the screening of electrostatic interactions between charged colloidal particles. Such a scenario is relevant for an experimental system used recently to investigate the effective forces acting on spherical particles close to a substrate immersed in a near-critical water-lutidine mixture [7,8]. The aim of that study was to measure directly a critical Casimir force between a single spherical colloid and a flat surface. Polystyrene particles with high surface-charge density were used as colloids, and silica glass treated chemically to achieve the desired adsorption properties, which also carried some surface charge, was used as the substrate. Ions in solution were present due to dissociation in the salt-free water-lutidine mixture. In order to extract the critical Casimir force from the measured potentials of interactions, the distances z from the substrate for which the electrostatic contribution was estimated to be negligible have been considered. The estimation of the electrostatic interactions was based on measurements of the electrostatic potential far from the critical point. However, different solubilities of ions in water and lutidine and the enhancement of one of components of the near-critical mixture close to the surfaces might result in a change in the screening of the electrostatic interaction compared to the case of a noncritical homogeneous medium. Unfortunately, possible effects of the critical adsorption on the electrostatic contribution to the interaction potential could not be estimated due to the lack of any theoretical predictions for such effects. Motivated by these issues in the present paper we study critical adsorption in a simple generic system, i.e., for a binary mixture solvent containing ionic solutes in the presence of a single charged planar wall that preferentially adsorbs one component of the solvent.

Recently, the properties of *bulk* near-critical binary mixtures with ions have been studied theoretically using a modified Poisson-Boltzmann theory by Onuki and Kitamura [9]. The Landau-Ginzburg functional was used to describe the binary solvent. The presence of ions was accounted for by including electrostatic contribution and the terms due to the entropy of ions. Preferential solvation effects were modeled by a linear coupling between the density of ions and the order parameter of near-critical binary mixture. Using this phenomenological functional in the mean-field approximation, the authors found that the presence of ions shifts the critical point of demixing. This result is consistent with the well known experimental observations that adding salt to the binary mixture solvent changes the position of its phase separation curve, such that the upper and lower critical

points are shifted upward [10,11] and downward [12], respectively.

If the ion-containing mixtures are exposed to external electric fields, e.g., due to charged walls or charged macromolecules immersed in the solution, the phase separation temperature is also shifted [13]. In addition to the preferential solvation, a dielectric inhomogeneity is important for this effect; the high permittivity solvent component is attracted to the charged surface thus enhancing the phase separation. Recently, the effects of these, so called, dielectrophoretic forces and of the preferential solvation have been studied for ion-containing mixtures confined between two-charged surfaces in a single phase region *away* from the coexistence [14]. The approach used for a bulk system in Ref. [9] have been modified to account for a spatial variation in the volume fractions and, consequently, of the dielectric permittivity of the binary mixture. In addition, a surface term describing the interactions between the charged solutes and confining charged surfaces has been included. Using a mean-field approximation the density profiles and osmotic pressure between charged interfaces have been calculated.

In order to investigate the influence of critical adsorption of ion-containing binary mixtures on the distribution of ions near a single charged wall, we propose here an approach that starts from the microscopic theory. Within such an approach the Landau functional is derived rather than postulated, and it should describe correctly all the collective phenomena in the system that are consistent with the assumed interaction potentials. Hence, we can control all the assumptions on the fundamental level of interactions. In Sec. II A we introduce the lattice-gas model of a four-component mixture describing two species of the solvent and the positive and negative ions. The generic for this model, short-ranged interactions between all the species and between the species and the surface are assumed. From the lattice model we derive the continuum Landau-Ginzburg functional which is then supplemented by electrostatic bulk and surface contributions. Contrary to previous approaches all parameters of our functional are expressed in terms of microscopic interactions. Our Landau functional is similar to the functionals in Refs. [9,14], but more terms are present, and all the approximations are based on assumptions concerning types of interparticle interactions. In Sec. II B we derive Euler-Lagrange (EL) equations that allow to calculate the density and charge profiles on a mean-field level. Next, in Sec. III we solve the linearized EL equations (Sec. III A) and calculate the leading-order correction to them (Sec. III B) under the assumption of weak interactions with the surface, small amount of ions and weak surface charge. A discussion of our results is included. The summary and outlook are given in Sec. IV.

II. DERIVATION OF THE LANDAU THEORY

A. Construction of the lattice model

Let us consider a two-component mixture approaching the upper critical point of the demixing transition from the one-phase side and investigate the effect of the presence of a small amount of positively and negatively charged ionic solutes. We are interested in such a system in contact with a charged wall, such that the total charge of the system neutralizes the charge at the wall. Let us first consider this system with the ions replaced by the corresponding neutral molecules. The electrostatic contribution to the free energy will be included in the next step.

The four-component mixture close to the demixing transition can be conveniently studied in the framework of the lattice-gas model. We consider a simple cubic lattice (SC) with the unit cell of the volume v_0. Here we limit ourselves to a mixture of molecules of similar sizes. The cell-occupancy operators are $\hat{o}_i(\mathbf{x})=1$ if the cell $\mathbf{x}$ is occupied by the ith component and $\hat{o}_i(\mathbf{x})=0$ otherwise. The two components of the solvent are denoted by $i=1,2$, and two additional species that can be ionized to carry positive or negative charges are indicated by $i=3,4$, respectively. We restrict ourselves to thermodynamic conditions corresponding to the stability of a liquid, where total density fluctuations can be neglected. The single-state occupancy and close-packing lead to the constraint

$$\sum_{i=1}^{4} \hat{o}_i(\mathbf{x}) = 1. \tag{1}$$

We consider an open system with the Hamiltonian (the electrostatic interactions are disregarded at this stage)

$$H^{SR}\{[\hat{o}_i(\mathbf{x})]\} = \mathcal{E}^{SR}\{[\hat{o}_i(\mathbf{x})]\} - \mu_1 \sum_{\mathbf{x}} \hat{o}_1(\mathbf{x}) - \mu_2 \sum_{\mathbf{x}} \hat{o}_2(\mathbf{x}) - \mu_3 \sum_{\mathbf{x}} [\hat{o}_3(\mathbf{x}) + \hat{o}_4(\mathbf{x})], \tag{2}$$

where $\beta=(k_BT)^{-1}$, k_B is the Boltzmann constant and T the temperature. μ_i is the chemical potential of the species i. We shall require charge neutrality for ionized species 3 and 4 in the bulk, and assume $\mu_3=\mu_4$. For the short-range interaction energy we make the standard nearest-neighbor (NN) approximation for all the species

$$\mathcal{E}^{SR}[\{\hat{o}_i(\mathbf{x})\}] = -\sum_{\mathbf{x}} \sum_{n=1}^{3} \hat{o}_i(\mathbf{x}) J_{ij} \hat{o}_j(\mathbf{x}+\hat{\mathbf{e}}_n), \tag{3}$$

where $\hat{\mathbf{e}}_n$ is the unit lattice vector in the nth direction and summation convention is used for $i,j=1,\ldots,4$. The coupling constants are symmetric, $J_{ij}=J_{ji}$, and represent the sum of all short-range interactions. We further assume that the species 3 and 4 are similar, i.e., interact in a similar way with the solvent and with each other, such that we can take

$$J_{33} + J_{44} \approx 2J_{34},$$

$$J_{13} \approx J_{14},$$

$$J_{23} \approx J_{24}. \tag{4}$$

With this assumption the Hamiltonian takes the form

$$\mathcal{H}^{SR}[\hat{s},\hat{\phi}^2] = -\sum_{\mathbf{x}\in V}\sum_{n=1}^{3}[\hat{s}(\mathbf{x})J_{ss}\hat{s}(\mathbf{x}+\mathbf{e}_n) + \hat{\phi}^2(\mathbf{x})J_{\rho\rho}\hat{\phi}^2(\mathbf{x}+\mathbf{e}_n) + \hat{s}(\mathbf{x})J_{s\rho}\hat{\phi}^2(\mathbf{x}+\mathbf{e}_n) + \hat{\phi}^2(\mathbf{x})J_{s\rho}\hat{s}(\mathbf{x}+\mathbf{e}_n)] - \sum_{\mathbf{x}\in V}[\Delta\mu\hat{s}(\mathbf{x}) + \Delta\mu_c\hat{\phi}^2(\mathbf{x})] - \sum_{\mathbf{x}\in\partial V}[h_s\hat{s}(\mathbf{x}) + h_\rho\hat{\phi}^2(\mathbf{x})]. \quad (5)$$

The system volume is denoted by V, ∂V denotes the boundary layer. The operators $\hat{s}$, $\hat{\phi}$, and $\hat{\phi}^2$ are defined as

$$\hat{s} = \hat{o}_1 - \hat{o}_2 = -1,0,1,$$

$$\hat{\phi} = \hat{o}_3 - \hat{o}_4 = -1,0,1,$$

$$\hat{\phi}^2 = \hat{o}_3 + \hat{o}_4 = 0,1. \quad (6)$$

From close packing [Eq. (1)] it follows that $\hat{o}_1+\hat{o}_2=\hat{s}^2=1-\hat{\phi}^2$. The coupling constants in Eq. (5) are linear combinations of the coupling constants J_{ij}, and $\Delta\mu$ and $\Delta\mu_c$ are linear combinations of μ_i. Note that the SR contribution to the energy depends only on $\hat{\phi}^2$ when the assumptions (4) are valid; otherwise the full expression consisting of terms linear in $\hat{\phi}$ has to be considered. We assume $J_{ss} \gg J_{\rho\rho}$, so that the system can phase separate into two phases, one of them rich in the first- and the other one rich in the second component of the solvent, rather than into a phase rich in the third component and a phase rich in the fourth component of the mixture. The coupling $J_{s\rho}>0$ signals that ions preferentially dissolve in the first component of the solvent.

When the species 3 and 4 are charged, then Coulomb interactions between them are present in addition to the short-range interactions. In the truly microscopic model one should take into account polarizability of the solvent, and the problem becomes very difficult. In the semimicroscopic description the effect of polarizability of the solvent is included only through the dielectric permittivity. The dielectric permittivity depends on the composition and, in the case of spatial inhomogeneities of the composition, the dielectric permittivity is a functional of the solvent densities and depends on $\mathbf{x}$. The electrostatic energy-density e_e in this case has the form [9,15]

$$e_e[s(\mathbf{x}),\rho_c(\mathbf{x}),\hat{\phi}(\mathbf{x}),\psi(\mathbf{x})] = \left[-\frac{\epsilon(\mathbf{x})}{8\pi}(\nabla\psi)^2 + e\hat{\phi}(\mathbf{x})\psi(\mathbf{x})\right], \quad (7)$$

where

$$s(\mathbf{x}) = \langle\hat{s}(\mathbf{x})\rangle, \quad \rho_c(\mathbf{x}) = \langle\hat{\phi}^2(\mathbf{x})\rangle \quad (8)$$

are the mean values of the microscopic operators, ∇ is the gradient and ψ is the electrostatic potential that in equilibrium corresponds to the minimum of the energy [Eq. (7)], i.e., to generalization of the Poisson equation, considered for example in Ref. [9]. Close to the demixing point of the binary mixture the densities vary on the length scale of the bulk correlation length $\xi_b \gg v_0^{1/3}$, and their deviations from the average value are small. It is then reasonable to assume that $\epsilon(\mathbf{x})$ is a linear function of the average densities of the two components of the solvent

$$\epsilon(\mathbf{x}) = \epsilon_1\rho_1(\mathbf{x}) + \epsilon_2\rho_2(\mathbf{x}), \quad (9)$$

where $\rho_1(\mathbf{x})=\langle\hat{o}_1(\mathbf{x})\rangle=(1/2)[1-\rho_c(\mathbf{x})+s(\mathbf{x})]$ and $\rho_2(\mathbf{x})=\langle\hat{o}_2(\mathbf{x})\rangle=(1/2)[1-\rho_c(\mathbf{x})-s(\mathbf{x})]$. ϵ_1 and ϵ_2 are the dielectric constants of the pure species 1 and 2, respectively. When the electrostatic energy has the above form, the average densities have to be determined self-consistently.

If one assumes, however, that $\epsilon(\mathbf{x})$ can be approximated by its average value

$$\epsilon(\mathbf{x}) \approx \bar{\epsilon}, \quad (10)$$

then the electrostatic energy (7) has the same form as in vacuum (with the modified permittivity) and can be written as a sum of interaction energies for all pairs of point charges,

$$\mathcal{E}^C[\{\hat{o}_i(\mathbf{x})\}] = \frac{1}{2}\sum_{\mathbf{x}}\sum_{\mathbf{x}'\neq\mathbf{x}}\sum_{i,j=3,4} e_i\hat{o}_i(\mathbf{x})V_c(|\mathbf{x}-\mathbf{x}'|)e_j\hat{o}_j(\mathbf{x}'), \quad (11)$$

where e_3 and e_4 are the charges, and V_c is the electrostatic interaction potential, which has the form different for different lattices and in the continuum space. The forms of V_c for simple cubic, body centered, or face centered lattices in the Fourier representation can be found, for example, in Refs. [16,17]. If we assume for V_c the continuum-space form and restrict the positions of ions to the lattice sites, then the electrostatic energy takes the familiar form of the sum of Coulomb interaction potential for all the pairs of ions

$$\mathcal{E}^C[\{\hat{\phi}(\mathbf{x})\}] = \frac{e^2}{2}\sum_{\mathbf{x}}\sum_{\mathbf{x}'\neq\mathbf{x}}\frac{\hat{\phi}(\mathbf{x})\hat{\phi}(\mathbf{x}')}{\bar{\epsilon}|\mathbf{x}-\mathbf{x}'|}. \quad (12)$$

In the above expression we limit ourselves to monovalent ions $e_3=-e_4=e$, with e denoting the elementary charge. With the above form of the electrostatic energy we obtain a well-defined semimicroscopic model with the probability distribution

$$p[\{\hat{s},\hat{\phi}\}] = \frac{\exp(-\beta\mathcal{H}[\{\hat{s},\hat{\phi}\}])\prod_{\mathbf{x}}\delta^{Kr}(\hat{s}^2+\hat{\phi}^2-1)}{\Xi}, \quad (13)$$

where $\mathcal{H}[\{\hat{s},\hat{\phi}\}]=\mathcal{H}^{SR}[\{\hat{s},\hat{\phi}^2\}]+\mathcal{E}^C[\{\hat{\phi}\}]$. The grand potential in the above statistical-mechanical model is given by

$$\Omega = -k_BT\ln\Xi. \quad (14)$$

The advantage of such kind of modeling with the assumption (10) is the possibility for investigating the effect of fluctuations of the composition (for example by means of computer simulations), and the disadvantage is neglecting the coupling between ϵ (and hence the electrostatic energy of states $\{\hat{o}_i\}$) and the composition fluctuations. Which effect, the fluctuations of the composition and their coupling to the density of ions or the spatial variation in ϵ, plays the dominant role in determining the charge distribution near the charged wall in a

system exhibiting critical fluctuations of concentration, remains an open question.

B. Mean-field approximation and continuous Landau-type model

In the mean-field (MF) approximation the grand potential is assumed to correspond to the minimum of the functional,

$$\Omega^{MF}[s,\rho_c,\phi,\psi] = \mathcal{H}^{SR}[s,\rho_c] + \sum_{\mathbf{x}\in V} (e_e[s,\rho_c,\phi,\psi] + k_BTW[s,\rho_c,\phi]), \tag{15}$$

where the electrostatic energy density $e_e[s,\rho_c,\phi,\psi]$ is given by Eq. (7), and $-k_BW[s,\rho_c,\phi]$ is the entropy density. In this work we focus on the semi-infinite system, and assume the lattice-gas form (ideal mixing entropy)

$$\begin{aligned} W(z) = {} & \frac{1-\rho_c(z)+s(z)}{2}\ln\left(\frac{1-\rho_c(z)+s(z)}{2}\right) \\ & + \frac{1-\rho_c(z)-s(z)}{2}\ln\left(\frac{1-\rho_c(z)-s(z)}{2}\right) \\ & + \frac{\rho_c(z)+\phi(z)}{2}\ln\left(\frac{\rho_c(z)+\phi(z)}{2}\right) \\ & + \frac{\rho_c(z)-\phi(z)}{2}\ln\left(\frac{\rho_c(z)-\phi(z)}{2}\right), \end{aligned} \tag{16}$$

where we take into account the dependence of the fields on the distance z from the planar wall.

We are interested in thermodynamic conditions corresponding to stability of the uniform fluid close to the demixing transition. The equilibrium values of s and ρ_c in the bulk are the uniform solutions of the Euler-Lagrange (EL) equations obtained from the minimization of the bulk part of the functional (15); they are denoted by $\bar{s}$ and $\bar{\rho}_c$. From now on we focus on the deviations from the equilibrium fields

$$\vartheta(z) = s(z) - \bar{s} \tag{17}$$

$$\eta(z) = \rho_c(z) - \bar{\rho}_c. \tag{18}$$

On the MF level it is possible to take into account the dependence of the dielectric constant on the composition and we assume that ϵ given by Eq. (9) depends on the distance z from the planar wall according to

$$\epsilon(z) = \bar{\epsilon} + \delta\epsilon(z), \tag{19}$$

where

$$\delta\epsilon(\mathbf{x}) = \epsilon_\vartheta\vartheta(\mathbf{x}) - \epsilon_\eta\eta(\mathbf{x}), \tag{20}$$

and we introduced the notation

$$\epsilon_\vartheta = \frac{(\epsilon_1-\epsilon_2)}{2}, \tag{21}$$

$$\epsilon_\eta = \frac{(\epsilon_1+\epsilon_2)}{2}. \tag{22}$$

For very small fields ϑ and η, the second term in Eq. (19) is negligible compared to the first one. We shall keep this term in general formulas, valid for arbitrary deviations from bulk equilibrium densities.

The continuum-space Landau-Ginzburg (LG) functional for the fields $\vartheta(z)$ and $\eta(z)$ is defined as

$$A\mathcal{L}[\vartheta,\eta,\phi,\psi] = \Omega^{MF}[\bar{s}+\vartheta,\bar{\rho}_c+\eta,\phi,\psi] - \Omega^{MF}[\bar{s},\bar{\rho}_c,0,0], \tag{23}$$

where A is the area of the confining surface in the semi-infinite geometry. $\mathcal{L}[\vartheta,\eta,\phi,\psi]$ can be derived from the lattice model in a standard way. For example, one can follow the method described in detail in Ref. [18]. In short, in the first step EL equations on the lattice are derived, which contain contributions of the form $\nabla^2 f = f(z+1)+f(z-1)-2f(z)$ for $f=s,\rho_c$. For the boundary layer the effect of the missing neighbors is taken into account, and in this way surface EL equations are obtained. At the boundary layer both the bulk and the surface EL equations must be satisfied, and the difference of the two equations gives the corresponding boundary condition. From the continuous version of the EL equations ($\nabla^2 f \to d^2f/dz^2$) we derive the corresponding functional with the appropriate surface term that leads to the boundary conditions. We require that the boundary conditions contain lower-order derivatives than the bulk equations. An alternative derivation is described in Appendix. The functional obtained in this way has the form

$$\mathcal{L} = \int_0^\infty dz\left\{\frac{1}{2}\mathbf{v}^T(z)\mathbf{C}^0\mathbf{v}(z) + \frac{1}{2}\mathbf{v}'^T(z)\mathbf{J}\mathbf{v}'(z) + e_e + k_BTP\right\} + \frac{\mathbf{v}^T(0)\mathbf{J}\mathbf{v}(0)}{2} - \mathbf{h}\mathbf{v}(0) + e\sigma\psi(0), \tag{24}$$

where boldface capital letters denote matrices. The transpose of the columnar vectors $\mathbf{v}$ and $\mathbf{v}'$ are $\mathbf{v}^T(z)=(\vartheta(z),\eta(z))$ and $\mathbf{v}'^T(z)=(d\vartheta(z)/dz, d\eta(z)/dz)$ respectively. The elements of the matrix $\mathbf{C}^0=(C^0_{ij})_{i,j=1,2}$, where indices 1 and 2 correspond to s and ρ, respectively, are given by

$$C^0_{ss} = k_BT\frac{1-\bar{\rho}_c}{(1-\bar{\rho}_c)^2-\bar{s}^2} - 6J_{ss}, \tag{25}$$

$$C^0_{\rho\rho} = k_BT\left(\frac{1-\bar{\rho}_c}{(1-\bar{\rho}_c)^2-\bar{s}^2} + \frac{1}{\bar{\rho}_c}\right) - 6J_{\rho\rho}, \tag{26}$$

$$C^0_{s\rho} = C^0_{\rho s} = k_BT\frac{\bar{s}}{(1-\bar{\rho}_c)^2-\bar{s}^2} - 6J_{\rho s}. \tag{27}$$

The second matrix in Eq. (24) is $\mathbf{J}:=(J_{ij})_{i,j=1,2}$, again with indices 1 and 2 corresponding to s and ρ, respectively. The electrostatic energy-density e_e in the case of a fluctuating dielectric constant has the form (7). The linear surface fields $\mathbf{h}=(\bar{h}_s,\bar{h}_\rho)$ are

$$\bar{h}_s = h_s - J_{ss}\bar{s} - J_{s\rho}\bar{\rho}_c, \quad \bar{h}_\rho = h_\rho - J_{\rho\rho}\bar{\rho}_c - J_{\rho s}\bar{s}, \tag{28}$$

and P is obtained from the expansion of W about $s=\bar{s}$ and $\rho_c=\bar{\rho}_c$ with the linear and quadratic parts in the fields ϑ and η subtracted. The length unit is the lattice constant $v_0^{1/3}$, comparable with the molecular diameter. The last term describes

the electrostatic interaction with the uniformly charged surface possessing the surface-charge density $e\sigma$.

C. Spinodal surface and bulk correlation functions

In order to find the bulk correlation functions in the Gaussian approximation as well as the spinodal surface and the critical line of this model in MF, let us consider the Gaussian part of the LG functional in the bulk. In the Fourier representation we have,

$$\mathcal{L}_G = \int \frac{d\mathbf{k}}{(2\pi)^3}\frac{1}{2}\tilde{\mathbf{v}}^*(\mathbf{k})\tilde{\mathbf{C}}(k)\tilde{\mathbf{v}}(\mathbf{k}), \tag{29}$$

where $\tilde{\mathbf{v}}^*(\mathbf{k})=\tilde{\mathbf{v}}^T(-\mathbf{k})$, and

$$\tilde{\mathbf{C}}(k) = \mathbf{C}^0 + k^2\mathbf{J} = \mathbf{J}(\mathbf{J}^{-1}\mathbf{C}^0 + k^2\mathbf{I}). \tag{30}$$

The correlation functions for the fluctuations of the solvent composition ϑ and the density of ions η in the Fourier representation are given by the matrix $\tilde{\mathbf{G}}=\tilde{\mathbf{C}}^{-1}$. Each component of this matrix is inversely proportional to $\det(\mathbf{J}^{-1}\mathbf{C}^0+k^2\mathbf{I})=(\lambda_1^2+k^2)(\lambda_2^2+k^2)$, where λ_1^2 and λ_2^2 are the two eigenvalues of the matrix

$$\mathbf{M} = \mathbf{J}^{-1}\mathbf{C}^0 \tag{31}$$

and are given by

$$\lambda_{1,2}^2 = \frac{Tr\,\mathbf{M} \mp \sqrt{(Tr\,\mathbf{M})^2 - 4\,\det\mathbf{M}}}{2}. \tag{32}$$

The correlations are thus given by a linear combination of the two terms, $(\lambda_1^2+k^2)^{-1}$ and $(\lambda_2^2+k^2)^{-1}$. The asymptotic decay of correlations in real space is described by the inverse correlation length $\xi_b^{-1}=\min(\lambda_1,\lambda_2)$.

The uniform phase is stable in the range of parameters T, $\bar{s}$, and $\bar{\rho}_c$ such that $\det\tilde{\mathbf{C}}(k)>0$ for all $k<k_{max}$, where k_{max} is an upper cutoff on wave numbers $|\mathbf{k}|\le k_{max}=\pi/a$. a is usually identified with some appropriate microscopic length, e.g., the lattice spacing or the molecular diameter. Because $\det\tilde{\mathbf{C}}(k)=J\,\det(\mathbf{M}+k^2\mathbf{I})=J(\lambda_1^2+k^2)(\lambda_2^2+k^2)$ where

$$J = \det\mathbf{J} = J_{ss}J_{\rho\rho} - J_{s\rho}^2, \tag{33}$$

for the instability analysis we have to distinguish cases of positive and negative J.

If $J>0$, from the condition $\det\tilde{\mathbf{C}}(0)\ge 0$ (one-phase stability) we obtain after some algebra that $Tr\,\mathbf{M}\ge 0$ and $\lambda_1^2,\lambda_2^2>0$. In that case the instability of the uniform phase occurs at $k=0$ when

$$\det\tilde{\mathbf{C}}(0) = J\,\det\mathbf{M} = J\lambda_1^2\lambda_2^2 = 0 \quad \text{or} \quad \tilde{C}_{ss} = 0. \tag{34}$$

The condition $\tilde{C}_{ss}=0$ determines the instability for the case of the vanishing field η (the same concentration of ions in the phase-separated solvent). From Eq. (32) it follows that $\lambda_1^2\to 0^+$ so that the asymptotic inverse decay length is $1/\xi_b=\lambda_1$.

For $J<0$, on the other hand, the stability condition of the uniform phase, $\det\tilde{\mathbf{C}}(k)>0$, requires $\det(\mathbf{M}+k^2\mathbf{I})=(\lambda_1^2+k^2)(\lambda_2^2+k^2)<0$ for all $k<k_{max}$. In particular, the uniform phase is stable against macroscopic phase separation as long as $\lambda_1^2\lambda_2^2<0$. The model can describe phase separation into two uniform phases only when the boundary of stability of the uniform phase is associated with $k=0$, i.e., when upon decreasing temperature $(\lambda_1^2+k^2)(\lambda_2^2+k^2)$ changes sign first at $k=0$. In our case this means that $\lambda_1^2\lambda_2^2>(\lambda_1^2+k_{max}^2)(\lambda_2^2+k_{max}^2)$; the necessary condition for the above is $\lambda_1^2+\lambda_2^2<0$. This condition can only be satisfied when $Tr\,\mathbf{M}<0$, since in this case $\lambda_1^2<0$ and $\lambda_2^2\to 0^+$; hence, $1/\xi_b=\lambda_2$. Our model permits an instability at $0<k\le k_{max}$, which will lead to the modulated phase, for a set of parameters satisfying $J<0$ and $Tr\,\mathbf{M}>0$, since in this case $\lambda_1^2\to 0^-$ and $\lambda_2^2>0$. We will not consider such parameters in the current paper.

For a given composition, the spinodal surface $T_s(\bar{s},\bar{\rho}_c)$ is determined by the higher temperature satisfying the condition (34). The explicit relation between the temperature and the composition of the mixture that satisfies the first condition in Eq. (34), reads

$$(k_BT_s)^2 + k_BT_s[12J_{s\rho}\bar{s}\bar{\rho}_c - 6J_{ss}(1-\bar{\rho}_c-\bar{s}^2) - 6J_{\rho\rho}\bar{\rho}_c(1-\bar{\rho}_c)] + 36J\bar{\rho}_c((1-\bar{\rho}_c)^2-\bar{s}^2) = 0 \tag{35}$$

For $\bar{\rho}_c=0$ we have simply $k_BT_c=6J_{ss}$ and $\bar{s}_c=0$ in this model. For a very small amount of ions the shift of the critical temperature can be estimated from the derivative of T_s with respect to $\bar{\rho}_c$ at $\bar{s}=\bar{\rho}_c=0$. The derivative at that point is

$$\frac{dT_s}{d\bar{\rho}_c} = \frac{6(J_{s\rho}^2 - J_{ss}^2)}{J_{ss}}, \tag{36}$$

while the derivative at $\bar{s}=\bar{\rho}_c=0$ of k_BT satisfying $\tilde{C}_{ss}(0)=0$ is $-6J_{ss}$. Hence, Eq. (35) describes the actual instability at least for small amount of the solute. The critical temperature increases upon addition of ions when $J_{s\rho}-J_{ss}>0$. Experimentally addition of some salt leads to the increase of the temperature of the upper critical point [10,11]. Thus, if we require that this model describes the experimental situation on the MF level, we should assume that $J_{s\rho}-J_{ss}>0$. This condition, together with the earlier assumption $J_{ss}>J_{\rho\rho}$, leads to $J<J_{ss}^2-J_{s\rho}^2<0$. On the other hand, for $J>0$ the critical point decreases upon addition of salt, which is not consistent with the experimental observation. However, the present study is limited to MF approximation, and the effect of fluctuations on the critical point should be taken into account to draw definite conclusions. We shall consider both cases, $J>0$ and $J<0$, bearing in mind that in the latter case the parameters must satisfy the condition $Tr\,\mathbf{M}<0$.

D. Euler-Lagrange equations in semi-infinite system

Our goal is to determine the shape of the ion number and charge density profiles near the charged wall, therefore we need to consider the Euler-Lagrange equations corresponding to the minimum of the functional (24).

From $\delta\mathcal{L}/\delta\phi(z)=0$ we obtain

$$\phi(z) = -\rho_c(z)g(z), \tag{37}$$

where

$$g(z) = \tanh(\beta e \psi(z)). \tag{38}$$

Note that $-1 < g(z) < 1$. From the above we can obtain ψ as a Taylor series in ϕ and η, of odd orders in ϕ. The charge density can be eliminated by using Eq. (37), and after some algebra we obtain three EL equations for ϑ, η, and g,

$$\begin{aligned} J(\vartheta'' + 6\vartheta) = \frac{k_B T}{2}[&(J_{\rho\rho} + J_{\rho s})\ln(1 - \rho_c + s) \\ &+ (J_{\rho s} - J_{\rho\rho})\ln(1 - \rho_c - s) - 2J_{\rho s}\ln(\rho_c) \\ &- J_{\rho s}\ln(1 - g^2)] - J_{\rho\rho}\Delta\bar{\mu} + J_{s\rho}\Delta\bar{\mu}_c \end{aligned} \tag{39}$$

$$\begin{aligned} J(\eta'' + 6\eta) = -\frac{k_B T}{2}[&(J_{\rho s} + J_{ss})\ln(1 - \rho_c + s) \\ &+ (J_{ss} - J_{\rho s})\ln(1 - \rho_c - s) - 2J_{ss}\ln(\rho_c) \\ &- J_{ss}\ln(1 - g^2)] + J_{s\rho}\Delta\bar{\mu} - J_{ss}\Delta\bar{\mu}_c \end{aligned} \tag{40}$$

$$\begin{aligned} &g''(1 - g^2)(\bar{\epsilon} + \epsilon_\vartheta\vartheta - \epsilon_\eta\eta) + 2gg'^2(\bar{\epsilon} + \epsilon_\vartheta\vartheta - \epsilon_\eta\eta) \\ &+ g'(1 - g^2)(\epsilon_\vartheta\vartheta' - \epsilon_\eta\eta') - \frac{4\pi e^2\rho_c(1 - g^2)^2 g}{k_B T} = 0 \end{aligned} \tag{41}$$

where

$$\Delta\bar{\mu} = \Delta\mu + 6J_{ss}\bar{s} + 6J_{\rho s}\bar{\rho}_c = -\frac{k_B T}{2}\ln\left[\frac{1 - \bar{\rho}_c + \bar{s}}{1 - \bar{\rho}_c - \bar{s}}\right] \tag{42}$$

and

$$\Delta\bar{\mu}_c = \Delta\mu_c + 6J_{\rho\rho}\bar{\rho}_c + 6J_{\rho s}\bar{s} = -\frac{k_B T}{2}\ln\left[\frac{\bar{\rho}_c^2}{(1 - \bar{\rho}_c)^2 - \bar{s}^2}\right]. \tag{43}$$

In the above equations we used the explicit lattice-gas expressions for the entropy (16). Equations for $\Delta\bar{\mu}$ and $\Delta\bar{\mu}_c$ follow from the bulk EL equations.

The boundary conditions of the EL equations for the functional (24) are

$$\frac{\bar{\epsilon} + \epsilon_\vartheta\vartheta(0) - \epsilon_\eta\eta(0)}{4\pi}\nabla\psi(z)|_{z=0} = -e\sigma \tag{44}$$

and

$$\vartheta' - \vartheta = H_\vartheta, \quad \eta' - \eta = H_\eta, \tag{45}$$

where

$$H_\vartheta = \frac{\bar{h}_\rho J_{\rho s} - \bar{h}_s J_{\rho\rho}}{J} = \bar{s} + \frac{h_\rho J_{\rho s} - h_s J_{\rho\rho}}{J},$$

$$H_\eta = \frac{\bar{h}_s J_{\rho s} - \bar{h}_\rho J_{ss}}{J} = \bar{\rho}_c + \frac{h_s J_{\rho s} - h_\rho J_{ss}}{J}. \tag{46}$$

J is defined in Eq. (33).

When $\epsilon = \bar{\epsilon}$, the third EL simplifies,

$$(1 - g(z)^2)g''(z)\bar{\epsilon} + 2g'^2 g(z)\bar{\epsilon} - \frac{4\pi e^2\rho_c(z)g(z)(1 - g(z)^2)^2}{k_B T} = 0 \tag{47}$$

Alternatively, ψ could be eliminated, and three EL equations for the fields ϑ, η and ϕ would be obtained.

III. APPROXIMATE SOLUTIONS OF THE EL EQUATIONS

The nonlinear EL Eqs. (39)–(45) can be solved numerically. Since in the critical region and for weak surface fields and small σ the magnitudes of the fields ϕ, ϑ, and η are small, we can obtain approximate analytical solutions within the perturbation method. Analytical solutions can give more general insight, but in the future studies should be supplemented with numerical solutions for particular choices of model parameters.

We postulate that the solutions of the EL equations can be written in the form

$$f = \sum_{n=1}^{N} f^{(n)} \tag{48}$$

where $f = \vartheta, \eta, \phi, \psi$, $f^{(n)} = O(\nu^n)$, and ν is a small parameter.

A. Solution of the linearized EL equations

Let us first consider the linearized Eqs. (39)–(41). For the linearized equations we shall simplify the notation, $\vartheta^{(1)} \equiv \vartheta$, $\eta^{(1)} \equiv \eta$, $\phi^{(1)} \equiv \phi$. For the electrostatic part we obtain the linearized equations of the well known form (the spatial dependence of permittivity leads to nonlinear contributions to the EL equations)

$$\frac{\bar{\epsilon}}{4\pi}\frac{d^2\psi(z)}{dz^2} + e\phi(z) = 0, \tag{49}$$

$$e\psi(z) + \frac{k_B T\phi(z)}{\bar{\rho}_c} = 0, \tag{50}$$

which together give

$$\phi(z)'' = \kappa^2\phi(z), \tag{51}$$

where

$$\kappa^2 = \frac{4\pi e^2\bar{\rho}_c}{k_B T\bar{\epsilon}}. \tag{52}$$

Note that κ is the inverse Debye length in units of the molecular size. Solution of Eq. (51) with the boundary condition Eq. (44) has the well known form

$$\phi(z) = -\kappa\sigma e^{-\kappa z}. \tag{53}$$

The equations for (η, ϑ) are formally the same as in the Landau theory for a mixture near the demixing critical point, and can be written in the form

$$\mathbf{v}'' = \mathbf{M}\mathbf{v} \tag{54}$$

where the matrix $\mathbf{M} = (M_{ij})$ with the indices 1 and 2 corresponding to s and ρ respectively, is defined in Eq. (31), and

the vector $\mathbf{v}$ is defined below Eq. (24). In the semi-infinite systems in the one-phase state $\vartheta(z), \eta(z) \to 0$ for $z \to \infty$, and from the Ansatz,

$$\vartheta = t_1 \exp(-\lambda_1 z) + t_2 \exp(-\lambda_2 z), \tag{55}$$

$$\eta = \bar{n} \exp(-\lambda_1 z) + n_2 \exp(-\lambda_2 z), \tag{56}$$

we obtain

$$\frac{t_i}{n_i} = \frac{\lambda_i^2 - M_{22}}{M_{21}}. \tag{57}$$

For $T \to T_c$ we have $1/\xi_b \to 0$ where $1/\xi_b = \lambda_1$ or $1/\xi_b = \lambda_2$ for $J > 0$ or $J < 0$ respectively (see Sec. II C), and the Eqs. (55) take the form

$$\vartheta(z) \simeq t_1 \exp(-z/\xi_b), \tag{58}$$

$$\eta(z) \simeq \bar{n} \exp(-z/\xi_b). \tag{59}$$

From the boundary conditions and Eq. (57) we obtain in this case

$$\bar{n} \simeq_{T \to T_c} - \frac{(H_\eta M_{11} - H_\vartheta M_{21})}{Tr\, \mathbf{M}} + \cdots, \tag{60}$$

$$t_1 \simeq_{T \to T_c} - \bar{n} \frac{M_{22}}{M_{21}} + \cdots. \tag{61}$$

Note that the linearized equations for ϕ and (η, ϑ) are decoupled. Thus, at the linear order there is no effect of the concentration profile on the charge distribution. Similar result was obtained recently in Ref. [19]. Note, however that we consider a simplified model of SR interactions, Eq. (5), where direct SR couplings between the charge and the concentration are disregarded.

B. Leading-order correction to the linearized EL equations

Beyond the linear order the coupling between the EL equations leads to modifications of the charge and concentration profiles. Note that the solution of the nonlinear equations can be written in the form (48) when all amplitudes of the solutions of the linearized equations are small and of the same order, $\kappa\sigma = O(\nu)$, $n_i = O(\nu)$ and $t_i = O(\nu)$. This means large Debye screening length and small surface-charge density, as well as weak surface fields H_η, H_θ [see Eqs. (60) and (61)]. We shall limit ourselves to such conditions and calculate the first correction $\vartheta^{(2)}$, $\eta^{(2)}$, $\phi^{(2)}$ to the solutions of the linearized equations.

For the electrostatic part we obtain

$$\psi^{(2)} = \frac{k_B T}{e \bar{\rho}_c} \left[\frac{\phi \eta}{\bar{\rho}_c} - \phi^{(2)} \right] \tag{62}$$

and

$$-(\phi^{(2)})'' + \kappa^2 \phi^{(2)} + \mathcal{N}_\phi(z) = 0, \tag{63}$$

where

$$\mathcal{N}_\phi(z) = \frac{\kappa^2}{4\pi e} [(\epsilon_\vartheta \vartheta'(z) - \epsilon_\eta \eta'(z)) \psi'(z) + (\epsilon_\vartheta \vartheta(z) - \epsilon_\eta \eta(z)) \psi''(z)] + (\phi(z) \bar{\eta}(z))'' \tag{64}$$

where we introduced $\bar{\eta}(z) = \eta(z)/\bar{\rho}_c = \bar{n}_1 \exp(-z/\xi_b)$, with $\bar{n}_1 = n_1/\bar{\rho}_c$. Note that at the second order in the perturbation expansion we need to calculate the function $\mathcal{N}_\phi$ to the quadratic order in ν. The first term in Eq. (64) is of the order $O(\nu^2 \kappa^2)$ [recall that we limit ourselves to boundary conditions such that the fields ϑ, η, ϕ obtained from linearized equations are all of the order of $O(\nu)$]. The perturbation expansion (48) is justified when $\kappa\sigma = O(\nu)$ [see Eq. (53)], i.e., for small surface charge and/or weak screening. When the additional condition, namely, $\kappa^2 \ll 1$ is satisfied (weak screening), the first term in Eq. (64) is negligible compared to the second one. In this case of weak screening the position dependence of the dielectric constant does not play a dominant role for the leading-order correction to the solution of the linearized EL equations, and we may assume $\epsilon = \bar{\epsilon}$. From the forms of the fields ϑ, η, ϕ obtained from linearized equations we obtain the explicit expression for $\mathcal{N}_\phi(z)$, and Eq. (63) simplifies to

$$-(\phi^{(2)})'' + \kappa^2 \phi^{(2)} - \kappa\sigma e^{-\kappa z} [(1/\xi_b + \kappa)^2 \bar{n}_1 e^{-z/\xi_b}] = 0. \tag{65}$$

The solution is

$$\phi^{(2)}(z) = \mathcal{A}_0 e^{-\kappa z} + \mathcal{A} \xi_b e^{-(\kappa + 1/\xi_b) z}, \tag{66}$$

where

$$\mathcal{A} = - \frac{\kappa\sigma \bar{n}_1 (\xi_b^{-1} + \kappa)^2}{(\xi_b^{-1} + 2\kappa)} \tag{67}$$

and $\mathcal{A}_0$ can be determined from the electroneutrality condition,

$$\int_0^\infty dz [\phi^{(1)}(z) + \phi^{(2)}(z)] + \sigma = 0. \tag{68}$$

The above condition is satisfied by the solution (53) of the linearized equation, hence for the correction term we have the condition $\int_0^\infty dz \phi^{(2)}(z) = 0$ that yields

$$\mathcal{A}_0 = - \kappa \frac{\mathcal{A} \xi_b}{(\kappa + \xi_b^{-1})}. \tag{69}$$

In the critical region $\xi_b^{-1} \to 0$, hence $\mathcal{A} \xi_b \to \infty$. However, $\phi^{(2)}(z)$ can be written in the following form:

$$\phi^{(2)}(z) = \bar{\mathcal{A}}_0 e^{-\kappa z} + \frac{\kappa\sigma \bar{n}_1 (\xi_b^{-1} + \kappa)^2}{(\xi_b^{-1} + 2\kappa)} e^{-\kappa z} \frac{(1 - e^{-z/\xi_b})}{\xi_b^{-1}}, \tag{70}$$

where

$$\bar{\mathcal{A}}_0 = - \kappa\sigma \frac{\bar{n}_1 (1 + \xi_b \kappa)}{1 + 2\xi_b \kappa}. \tag{71}$$

Thus, $\phi^{(2)}(z)$ is regular for $\xi_b^{-1} \to 0$. However, coupling between the concentration and the charge fluctuations in the functional (24) leads to the correction term in (70) which is

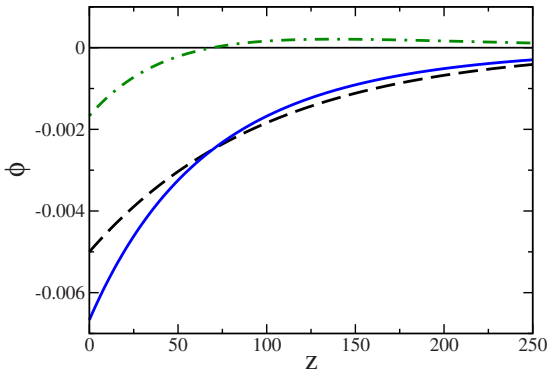

FIG. 1. (Color online) Charge density profiles in the semi-infinite system. The dashed line is the solution of the linearized Eq. (53), $\phi^{(1)}(z)$, the dash-dotted line is the correction term (72), $\phi^{(2)}(z)$, and the solid line is the sum of the two functions, $\phi^{(1)}(z)+\phi^{(2)}(z)$, for $\kappa=0.01$, $\sigma=0.5$, $\xi_b=100$, and $\bar{n}_1=0.5$. The charge density is in e/v_0 units, where e is the elementary charge, and z is in $v_0^{1/3}$ units, where v_0 is the volume per molecule in the close-packed system and we assume that all molecules are of similar size.

nonmonotonic as a function of z. The ratio between the correction and the leading-order term has the form

$$\frac{\phi^{(2)}(z)}{\phi^{(1)}(z)} \approx \frac{\bar{n}_1(1+\xi_b\kappa)}{1+2\xi_b\kappa}R(z), \tag{72}$$

where

$$R(z) = 1-(1+\xi_b\kappa)(1-e^{-z/\xi_b}) = \mathcal{R}(z^*,\xi_b\kappa)$$
$$= 1-(1+\xi_b\kappa)(1-e^{-z^*/\xi_b\kappa}) \tag{73}$$

is independent of the amplitude $\bar{n}_1$, and as a function of dimensionless distance $z^*=\kappa z$ depends only on the ratio between the relevant length scales, $\xi_b\kappa$. The nonmonotonic correction to the linear solution of the EL equations assumes an extremum at [compare Eq. (73)]

$$\kappa z_{extr} = 2\kappa\xi_b \ln\left(\frac{\kappa\xi_b+1}{\kappa\xi_b}\right). \tag{74}$$

From Eq. (72) it follows that the correction term changes its sign at $z_0=z_{extr}/2$. This is illustrated in Figs. 1 and 2 for the case when the Debye screening length κ^{-1} is equal to the

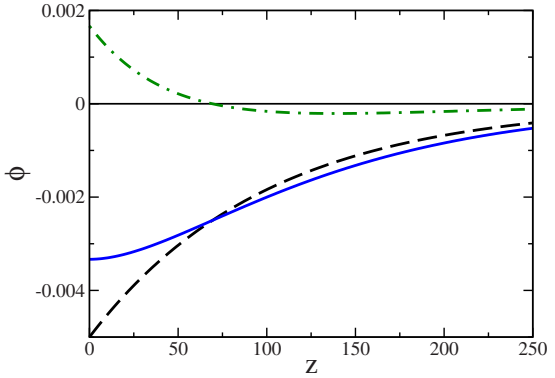

FIG. 2. (Color online) The same as in Fig. 1 but for $\bar{n}_1=-0.5$.

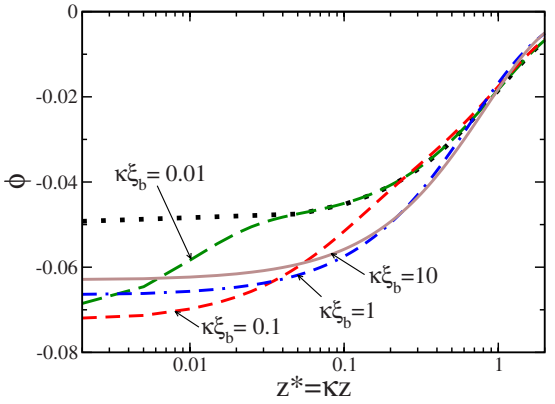

FIG. 3. (Color online) Charge density profiles as a function of the scaled distance $z^*=\kappa z$ for several values of the variable $\kappa\xi_b$ as indicated in the plot. The dotted line is the solution of the linearized Eq. (53), $\phi^{(1)}(z)$. Here, $\kappa\sigma=0.05$ and $\bar{n}_1=0.5$. The curve for $\kappa\xi_b=100$ coincides with the curve for $\kappa\xi_b=10$.

correlation length ξ_b. The critical adsorption for $z<z_0$ leads to the charge density *larger* than that predicted by the Debye-Hückel theory for $\bar{n}_1>0$, whereas for $z>z_0$ the charge density is *smaller* (see Fig. 1). Since $\int_0^\infty dz\phi(z)=-\sigma$, the enhanced charge density near the surface must lead to the depleted density away from the surface compared to the solution of the linearized equation. Thus, as a result of the critical adsorption of the component that is preferred by the ions, the screening length is effectively shorter. On the other hand, for $\bar{n}_1<0$ the charge density is *smaller* than that predicted by the Debye-Hückel theory at distances $z<z_0$, whereas for $z>z_0$ the charge density is *larger* (see Fig. 2). In this case the screening length is effectively larger than predicted by the Debye-Hückel theory. The effect is proportional to the amplitude $\bar{n}_1$ of the deviation of the density of ions from the bulk value, $\rho_c(z)/\bar{\rho}_c-1\approx\bar{n}_1\exp(-z/\xi_b)$. Plots correspond to $|\bar{n}_1|=0.5$.

To further illustrate this trend we note that the charge profile can be written in the scaling form

$$\phi(z) = -\kappa\sigma e^{-z^*}\Phi(z^*;\kappa\xi_b,\bar{n}_1), \tag{75}$$

where $\Phi(z^*;\kappa\xi_b,\bar{n}_1)$ is the scaling function, and we show in Fig. 3 the profiles for different values of $\kappa\xi_b$ and for $\bar{n}_1=0.5$. For smaller values of the product $\kappa\xi_b$ the profile is much enhanced near the surface, i.e., for $z^*\lesssim 0.2$, but decays quickly with the scaled distance z^* from the surface, whereas for larger values of $\kappa\xi_b$ the profile is less enhanced at the surface but decays slower with z^* for distances $z^*\lesssim 1$. More generally, from Eqs. (72) and (73) it follows that the value at the surface, $\phi(0)$, changes from $\phi(0)=-\kappa\sigma(1+\bar{n}_1)$ for $\kappa\xi_b\to 0$ to $\phi(0)=-\kappa\sigma(1+\bar{n}_1/2)$ for $\kappa\xi_b\to\infty$. For fixed $z^*\gtrsim 1$ (not shown in Fig. 3 for clarity), the absolute value of the charge density decreases for increasing $\kappa\xi_b$.

Let us consider the nonmonotonic correction term for the two limiting cases, $\kappa\xi_b\ll 1$ and $\kappa\xi_b\gg 1$ in more detail. For $\kappa\ll\xi_b^{-1}$, i.e., away from the critical point, from Eq. (72) it follows that it has a simple exponential form with the amplitude equal to the amplitude $\bar{n}_1$,

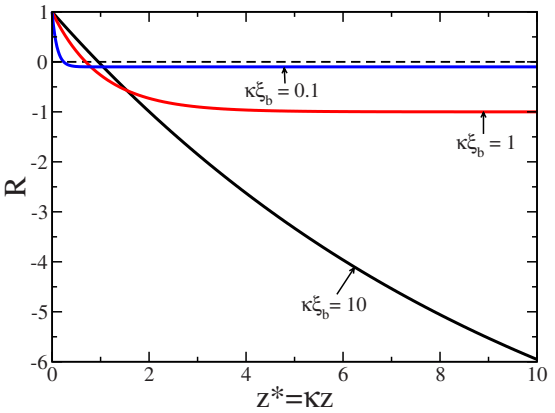

FIG. 4. (Color online) The rescaled ratio R (Eq. (73)) between the leading-order correction (72) and the Debye-Hückel form (53) of the charge density profile as a function of the scaled distance $z^*=\kappa z$ for several choices of the product $(\kappa\xi_b)$ as indicated in the plot.

$$\phi^{(2)}(z)/\phi^{(1)}(z) \approx \bar{n}_1 e^{-z/\xi_b} \quad \kappa \ll \xi_b^{-1}. \tag{76}$$

In this case the correction term is negligible for experimentally relevant distances $z^* > \kappa\xi_b$, as shown in Fig. 3 for $\kappa\xi_b \leq 0.1$.

For $T \to T_c$ we have $\xi_b^{-1} \to 0$, and using $\xi_b^{-1} \ll \kappa$ we obtain the approximation

$$\phi^{(2)}(z)/\phi^{(1)}(z) \simeq \frac{\bar{n}_1}{2}[1 - \kappa\xi_b(1 - e^{-z/\xi_b})] \quad \kappa \gg \xi_b^{-1}. \tag{77}$$

For $z \ll \xi_b$ the above takes the simple form

$$\phi^{(2)}(z)/\phi^{(1)}(z) \simeq \frac{\bar{n}_1}{2}[1 - \kappa z]. \tag{78}$$

The correction term changes sign for $\kappa z_0 \approx 1$, i.e., for sufficiently large correlation length the range of enhanced charge density in reduced units is independent of ξ_b.

It is instructive to examine the rescaled ratio R between the leading-order correction and the Debye-Hückel approximation which is independent of the surface parameters $\bar{n}_1$ and σ but displays the interplay between two length scales κ^{-1} and ξ_b in determining the strength of the correction term. R is shown in Fig. 4 as a function of the scaled distance $z^* = \kappa z$ for three different values of the product $\kappa\xi_b$. For $\kappa z \ll \kappa\xi_b$ we observe a linear decay of R in agreement with Eq. (78), whereas for $\kappa z \sim \kappa\xi_b$ an exponential decay to the value $-\kappa\xi_b$, at which R stabilizes for $\kappa z \gg \kappa\xi_b$, is observed.

Equations for the first corrections to the nonelectrostatic part read

$$(\mathbf{v}^{(2)})'' = \mathbf{M}\mathbf{v}^{(2)} + \mathbf{D}, \tag{79}$$

where $\mathbf{v}^{(2)} = (\vartheta^{(2)}, \eta^{(2)})$, and the components of the vector $\mathbf{D}^T = (D_s, D_\rho)$ are

$$D_s = \frac{D^a_{\vartheta\vartheta}\vartheta^2 + D^a_{\vartheta\eta}\vartheta\eta + D^a_{\eta\eta}\eta^2 + D^a_{\phi\phi}\phi^2}{J}, \tag{80}$$

$$D_\rho = \frac{D^b_{\vartheta\vartheta}\vartheta^2 + D^b_{\eta\vartheta}\vartheta\eta + D^b_{\eta\eta}\eta^2 + D^b_{\phi\phi}\phi^2}{J}. \tag{81}$$

As follows from Eq. (79) the correction terms to the composition profile $\vartheta(z)$ of the mixture are of the order of e^{-2z/ξ_b} and $e^{-2\kappa z}$. Note that the effect of the charges on the profiles of the composition of the mixture is negligible in the critical region, where $\kappa \gg \xi_b^{-1}$.

IV. SUMMARY AND OUTLOOK

Starting from the lattice-gas model of a four-component mixture we have derived the continuum Landau-Ginzburg model for binary mixture solvents in the presence of ions near the critical point of the demixing transition. The model encompasses the composition of the binary solvent field ϑ, the density of ions field η and the charge density field ϕ. It takes into account electrostatic interactions and the preferential solvation. The coupling constants appearing in this extended Landau-Ginzburg theory are given explicitly in terms of thermodynamic quantities, the temperature, the mean composition of solvent, the mean density of ions, and the interaction parameters J_{ij} characterizing the lattice-gas model of a mixture. We have assumed that ions are of similar chemical nature.

The main difference between our functional and the functional studied in Ref. [9] is the presence of the term $\propto \eta^2$ and terms $\propto (\nabla\eta)^2$ and $\propto \nabla\eta\nabla\vartheta$ in Eq. (24), which result from short-range interaction potentials. These terms lead to the mixing of the fields ϑ and η in the critical order parameter. In the semi-infinite system these terms are important for the form of the profile of the field η, and through the coupling of η with the charge density ϕ in the entropy term, they influence the charge profile $\phi(z)$. In our approach, direct couplings between the charge and the concentration are disregarded, but such coupling would be present in the case of ions of different chemical nature.

Mean-field theory for our Landau-Ginzburg model yields the shift of the critical point of the demixing transition with respect to the case of binary solvents without ions. The direction of the shift depends on the relative strength of the ions-solvent and solvent-solvent interaction parameters $J_{s\rho}$ and J_{ss}, and is positive for $J_{s\rho} > J_{ss}$. The linearized EL equations in the presence of a charged wall do not lead to the effect of the concentration profiles on the charge distribution. We treat nonlinear effects using a perturbation expansion, which gives the simple expression for the leading correction to the solution of the linearized EL Eqs. (72) and (73). The ratio between the next-to-leading and leading terms is proportional to the amplitude $\bar{n}_1$ of the decay of the ion density, $\bar{\eta} = \bar{n}_1 \exp(-z/\xi_b)$, and otherwise depends only on the dominant lengths in the system, the bulk correlation length ξ_b and the Debye screening length $1/\kappa$. We find that due to the critical adsorption of that component of the solvent in which the ions are preferentially dissolved, the amount of counterions in the layer near the charged surface of the thickness of the Debye screening length is increased with respect to the one away from the critical point. Critical adsorption of the better solvent enhances screening whereas the critical ad-

sorption of the poorer solvent leads to the opposite effect. This approach is quantitatively valid provided the Debye screening length is large, the surface-charge density is small, and the surface fields are weak. We expect the same trend beyond the approximate perturbation expansion solution. This will be studied further by the numerical treatment of the full EL equations.

We should note that our theory shows that the leading-order correction to the Debye-Hückel form of the charge profile is determined by the average dielectric constant, i.e., the spatial variation in the dielectric constant can be neglected when $\kappa \ll 1$ (in units of inverse molecular size).

Finally, the change in the charge distribution near the charged surface occurring upon approaching the critical point of the binary solvent, indicates that in the confining geometries, i.e., for systems between two surfaces, the effective interactions between the confining surfaces will be altered. Our predictions will be tested in the future work by explicit calculations and by comparison with the experimental data of Ref. [7].

ACKNOWLEDGMENTS

We would like to thank S. Dietrich, M. Bier, L. Helden and C. Bechinger for discussions. We also thank F. Pousaneh for careful reading of the manuscript. The work of AC was partially supported by the Polish Ministry of Science and Higher Education, Grant No. NN 202 006034.

APPENDIX: DERIVATION OF THE CONTINUUM FUNCTIONAL

The grand potential on the lattice in the MF approximation (15) is given by the explicit expression

$$\Omega^{MF} = \sum_{\mathbf{x}\in V} \omega_b^{MF}(\mathbf{x}) + \sum_{\mathbf{x}\in \partial V} \omega_s^{MF}(\mathbf{x}) \tag{A1}$$

with

$$\begin{aligned}\omega_b^{MF}(\mathbf{x}) = &-\Bigg[\frac{J_{ss}}{2}s(\mathbf{x})\Bigg(6s(\mathbf{x}) + \sum_{n=1}^{3}\nabla_n^2 s(\mathbf{x})\Bigg) + \frac{J_{\rho\rho}}{2}\rho_c(\mathbf{x}) \\ &\times\Bigg(6\rho_c(\mathbf{x}) + \sum_{n=1}^{3}\nabla_n^2\rho_c(\mathbf{x})\Bigg) + J_{s\rho}s(\mathbf{x})\Bigg(6\rho_c(\mathbf{x}) \\ &+ \sum_{n=1}^{3}\nabla_n^2\rho_c(\mathbf{x})\Bigg) + \Delta\mu s(\mathbf{x}) + \Delta\mu_c\rho_c(\mathbf{x})\Bigg] + e_e(\mathbf{x}) \\ &+ k_BTW(\mathbf{x})\end{aligned} \tag{A2}$$

and

$$\begin{aligned}\omega_s^{MF}(\mathbf{x}) = &- h_s s(\mathbf{x}) - h_\rho\rho_c(\mathbf{x}) + e\sigma\psi(\mathbf{x}) + J_{s\rho}s(\mathbf{x})[\rho_c(\mathbf{x}) \\ &- \nabla_3^-\rho_c(\mathbf{x})] + \frac{J_{ss}}{2}s(\mathbf{x})[s(\mathbf{x}) - \nabla_3^- s(\mathbf{x})] + \frac{J_{\rho\rho}}{2}\rho_c(\mathbf{x}) \\ &\times[\rho_c(\mathbf{x}) - \nabla_3^-\rho_c(\mathbf{x})],\end{aligned} \tag{A3}$$

where e_e is the electrostatic energy [Eq. (7)], $-k_BW(\mathbf{x})$ is the entropy density [Eq. (16)] which in general depends on $\mathbf{x}$, and we introduced lattice difference operators

$$\nabla_n^- f(\mathbf{x}) \equiv f(\mathbf{x}) - f(\mathbf{x} - \mathbf{e}_n), \tag{A4}$$

$$\nabla_n^+ f(\mathbf{x}) \equiv f(\mathbf{x} + \mathbf{e}_n) - f(\mathbf{x}), \tag{A5}$$

$$\nabla_n^2 f(\mathbf{x}) \equiv \nabla_n^+ f(\mathbf{x}) - \nabla_n^- f(\mathbf{x}) = f(\mathbf{x} + \mathbf{e}_n) + f(\mathbf{x} - \mathbf{e}_n) - 2f(\mathbf{x}), \tag{A6}$$

where $\mathbf{x}=(x_1,x_2,x_3)$, $\mathbf{e}_1=(1,0,0)$, $\mathbf{e}_2=(0,1,0)$, and $\mathbf{e}_3=(0,0,1)$. We assume that $\mathbf{x}\in\partial V$ when $\mathbf{x}=(x_1,x_2,0)$, i.e., at the boundary $x_3=0$. The last three surface terms compensate for the contribution from the missing neighbors at the surface that are present in the bulk term of this form, therefore should be subtracted.

For slowly varying functions we can approximate the sums by the integrals, and also make the approximations $\nabla_n^- f(\mathbf{x}) \approx \partial f(\mathbf{x})/\partial x_n$ and $\nabla_n^2 f(\mathbf{x}) \approx \partial^2 f(\mathbf{x})/\partial x_n^2$. Next, we can integrate by parts the term $s(\mathbf{x})\Sigma_{n=1}^3 \partial^2 s(\mathbf{x})/\partial x_n^2$, obtaining

$$\begin{aligned}-\frac{J_{ss}}{2}\int_{-\infty}^{\infty}dx_1\int_{-\infty}^{\infty}dx_2\int_0^{\infty}dx_3 s(\mathbf{x})\sum_{n=1}^{3}\frac{\partial^2 s(\mathbf{x})}{\partial x_n^2} = \\ + \frac{J_{ss}}{2}\int_{-\infty}^{\infty}dx_1\int_{-\infty}^{\infty}dx_2\int_0^{\infty}dx_3\sum_{n=1}^{3}\left(\frac{\partial s(\mathbf{x})}{\partial x_n}\right)^2 \\ - \frac{J_{ss}}{2}\int_{-\infty}^{\infty}dx_1\int_{-\infty}^{\infty}dx_2 s(x_1,x_2,0)\left.\frac{\partial s(x_1,x_2,x_3)}{\partial x_3}\right|_{x_3=0},\end{aligned} \tag{A7}$$

with similar result for the two remaining contributions in Eq. (A1) associated with inhomogeneous concentration. Note that the surface terms containing derivatives in the continuum version of the functional (A1) cancel against the surface terms that come from the integration by parts [see Eq. (A7)]. As a result we obtain for the semi-infinite system with the boundary at $x_3=0$,

$$\begin{aligned}\Omega^{MF} = &\int d\mathbf{R}\int_0^{\infty}dz\Bigg[\frac{J_{ss}}{2}\{-6s(\mathbf{x})^2 + [\nabla s(\mathbf{x})]^2\} + \frac{J_{\rho\rho}}{2}\{-6\rho_c(\mathbf{x})^2 \\ &+ [\nabla\rho_c(\mathbf{x})]^2\} + J_{\rho s}[-6\rho_c(\mathbf{x})s(\mathbf{x}) + \nabla s(\mathbf{x})\cdot\nabla\rho_c(\mathbf{x})] \\ &+ e_e(\mathbf{x}) + W(\mathbf{x}) - \Delta\mu s(\mathbf{x}) - \Delta\mu_c\rho_c(\mathbf{x})\Bigg] \\ &+ \int d\mathbf{R}\Bigg[-h_s s(\mathbf{R},0) - h_\rho\rho_c(\mathbf{R},0) + e\sigma\psi(\mathbf{R},0) \\ &+ J_{s\rho}s(\mathbf{R},0)\rho_c(\mathbf{R},0) + \frac{J_{ss}}{2}s(\mathbf{R},0)^2 + \frac{J_{\rho\rho}}{2}\rho_c(\mathbf{R},0)^2\Bigg]\end{aligned} \tag{A8}$$

where $\mathbf{R}=(x_1,x_2,0)$ and $x_3\equiv z$.

In the next step we consider the difference between the grand potential in the presence of the confining wall, and the grand potential in the bulk of the same volume. In the one-phase region the bulk is characterized by $\phi=\psi=0$, $s=\bar{s}$, and $\rho_c=\bar{\rho}_c$, which correspond to the minimum of the bulk part of the grand potential, $\Omega^{MF}(\bar{s},\bar{\rho}_c,0,0)=\int d\mathbf{x}\omega_b^{MF}(\bar{s},\bar{\rho}_c,0,0)$.

The excess grand potential $\Delta\Omega^{MF}(\vartheta+\bar{s},\eta+\bar{\rho}_c,\phi,\psi)=\Omega^{MF}(s,\rho_c,\phi,\psi)-\int d\mathbf{x}\omega_b^{MF}(\bar{s},\bar{\rho}_c,0,0)$ takes the form

$$\begin{aligned}\Delta\Omega^{MF}=&\int d\mathbf{R}\int_0^\infty dz\Bigg[\frac{J_{ss}}{2}(-6\vartheta(\mathbf{x})^2+(\nabla\vartheta(\mathbf{x}))^2)\\&+\frac{J_{\rho\rho}}{2}(-6\eta(\mathbf{x})^2+(\nabla\eta(\mathbf{x}))^2)\\&+J_{\rho s}(-6\eta(\mathbf{x})\vartheta(\mathbf{x})+\nabla\vartheta(\mathbf{x})\cdot\nabla\eta(\mathbf{x}))+e_e(\mathbf{x})\\&+k_BTP_1(\mathbf{x})\Bigg]+\int d\mathbf{R}\Bigg[-\bar{h}_s\vartheta(\mathbf{R},0)-\bar{h}_\rho\eta(\mathbf{R},0)\\&+e\sigma\psi(\mathbf{R},0)+\frac{J_{ss}}{2}\vartheta(\mathbf{R},0)^2\\&+\frac{J_{\rho\rho}}{2}\eta(\mathbf{R},0)^2+J_{s\rho}\vartheta(\mathbf{R},0)\eta(\mathbf{R},0)\Bigg]\\&+\int d\mathbf{R}\Bigg[-h_s\bar{s}-h_\rho\bar{\rho}_c+\frac{J_{ss}}{2}\bar{s}^2+\frac{J_{\rho\rho}}{2}\bar{\rho}_c^2+J_{s\rho}\bar{s}\bar{\rho}_c\Bigg].\end{aligned}\tag{A9}$$

The surface fields $\bar{h}_s$ and $\bar{h}_\rho$ are given in Eq. (28), P_1 is equal to $W(\mathbf{x})$ with the terms linear in the fields ϑ and η subtracted. Since in the bulk Ω^{MF} assumes minimum for vanishing fields ϕ, ψ, ϑ, and η, the bulk part of $\Delta\Omega^{MF}$ contains terms of second and higher order in these fields. The last five terms represent the constant contribution and can be neglected since they play no role for the shape of the fields ϕ, ϑ and η. Finally, when the fields depend only on the distance form the wall z, Eq. (A9) simplifies to the form (24).

[1] K. Binder, in *Phase Transitions and Critical Phenomena*, edited by C. Domb and J. L. Lebowitz (Academic, London, 1983), Vol. 8, p. 1.

[2] H. W. Diehl, in *Phase Transitions and Critical Phenomena*, edited by C. Domb and J. L. Lebowitz (Academic, London, 1986), Vol. 10, p. 76.

[3] M. E. Fisher and P. G. de Gennes, C. R. Seances Acad. Sci., Ser. B **287**, 207 (1978).

[4] *Supercritical Fluids—Fundamentals and Applications*, edited by E. Kiran, P. G. Debenedetti, and C. J. Peters, Proceedings of the NATO Advanced Study Institute, NATO Science Series E: Applied Science, Vol. 366, (Kluwer, Dordrecht, 2000).

[5] Y. Xia, B. Gates, Y. Yin, and Y. Lu, Adv. Mater. **12**, 693 (2000).

[6] J. N. Israelachvili, *Intermolecular and Surface Forces* (Academic, London, 1992).

[7] C. Hertlein, L. Helden, A. Gambassi, S. Dietrich, and C. Bechinger, Nature (London) **451**, 172 (2008).

[8] A. Gambassi, A. Maciolek, C. Hertlein, U. Nellen, L. Helden, C. Bechinger, and S. Dietrich, Phys. Rev. E **80**, 061143 (2009).

[9] A. Onuki and H. Kitamura, J. Chem. Phys. **121**, 3143 (2004).

[10] E. L. Eckfeldt and W. W. Lucasse, J. Phys. Chem. **47**, 164 (1943).

[11] B. J. Hales, G. L. Bertrand, and L. G. Hepler, J. Phys. Chem. **70**, 3970 (1966).

[12] V. Balevicius and H. Fuess, Phys. Chem. Chem. Phys. **1**, 1507 (1999).

[13] Y. Tsori and L. Leibler, Proc. Natl. Acad. Sci. U.S.A. **104**, 7348 (2007).

[14] D. Ben-Yaakov, D. Andelman, D. Harries, and R. Podgornik, J. Phys. Chem. B **113**, 6001 (2009).

[15] J. D. Jackson, *Classical Electrodynamics*, 3rd ed. (Academic, New York, 1999).

[16] A. Ciach and G. Stell, Phys. Rev. E **70**, 016114 (2004).

[17] A. Ciach and G. Stell, Int. J. Mod. Phys. B **19**, 3309 (2005).

[18] A. Ciach and V. Babin, J. Mol. Liq. **112**, 37 (2004).

[19] M. Bier and S. Dietrich (unpublished).